



REVISTA DE INGENIERIA DE LA FACULTAD DE INGENIERIA - UNIVERSIDAD NACIONAL DE COLOMBIA - BOGOTÁ

DYNA

ISSN: 0012-7353

Universidad Nacional de Colombia

Escobar, Freddy Humberto; Bonilla, Luis Fernando; Hernández, Claudia Marcela  
A practical calculation of the distance to a discontinuity in anisotropic systems from well test interpretation  
DYNA, vol. 85, no. 207, 2018, October-December, pp. 65-73  
Universidad Nacional de Colombia

DOI: <https://doi.org/10.15446/dyna.v85n207.72281>

Available in: <https://www.redalyc.org/articulo.oa?id=49658894009>

- How to cite
- Complete issue
- More information about this article
- Journal's webpage in redalyc.org

UNEN 

Scientific Information System Redalyc  
Network of Scientific Journals from Latin America and the Caribbean, Spain and  
Portugal

Project academic non-profit, developed under the open access initiative

# A practical calculation of the distance to a discontinuity in anisotropic systems from well test interpretation

Freddy Humberto Escobar<sup>a</sup>, Luis Fernando Bonilla<sup>a</sup> & Claudia Marcela Hernández<sup>b</sup>

<sup>a</sup> Grupo de Investigación GIPE, Facultad de Ingeniería, Universidad Surcolombiana, Neiva, Colombia. [fescobar@usco.edu.co](mailto:fescobar@usco.edu.co), [fernando.bonilla@usco.edu.co](mailto:fernando.bonilla@usco.edu.co),

<sup>b</sup> Ecopetrol, Bogotá, Colombia. [claudiama.hernandez@ecopetrol.com.co](mailto:claudiama.hernandez@ecopetrol.com.co)

Received: May 18<sup>th</sup> de 2018. Received in revised form: September 11<sup>th</sup>, 2018. Accepted: September 24<sup>th</sup>, 2018

## Abstract

Well testing is the cheapest and most accurate tool available to find the distance from a well to a linear constant-pressure boundary or fault. Several methods exist in the literature with which to determine this parameter. Most of them use conventional analysis and are only useful for isotropic reservoir systems. The few methods for anisotropic systems obtain the well-to-discontinuity distance through conventional analysis, type-curve matching and *TDS* technique, and then a correction by anisotropic effects is applied. In this work, a unified behavior of the pressure derivative was found, so the new shorter and most practical expressions used to find the distance from the well to the discontinuity, including the simultaneous effects of anisotropy angle and anisotropy index, are included. These new formulae were successfully tested with two synthetic examples and one field case example, and deviation errors higher than 30% are observed if an anisotropic system is treated as an isotropic one.

**Keywords:** anisotropy; linear boundary; fault; constant-pressure boundary.

# Cálculo práctico de la distancia a una discontinuidad en sistemas anisotrópicos a partir de la interpretación de pruebas de presión

## Resumen

Las pruebas de presión constituyen la herramienta más económica y precisa disponible para encontrar la distancia desde un pozo a un límite o falla de presión constante lineal. Existen varios métodos en la literatura para determinar este parámetro. La mayoría de ellos usa análisis convencionales y solo son útiles para sistemas de yacimientos isotrópicos. Los pocos métodos para sistemas anisotrópicos obtienen la distancia entre el pozo y la discontinuidad a través del análisis convencional, el ajuste de curvas de tipos y la técnica *TDS*, y luego se aplica una corrección por efectos anisotrópicos. En este trabajo, se encontró un comportamiento unificado de la derivada a presión, por lo que se incluyen las nuevas expresiones más cortas y prácticas para encontrar la distancia desde el pozo a la discontinuidad, incluidos los efectos simultáneos del ángulo de anisotropía y el índice de anisotropía. Estas nuevas fórmulas se probaron con éxito con dos ejemplos sintéticos y un ejemplo de caso de campo, y se observan errores de desviación superiores al 30% si un sistema anisotrópico se trata como si fuese un sistema isotrópico.


**Palabras Clave:** anisotropía; barrera lineal; falla; frontera a presión constante.

## 1. Introduction

Well testing is the cheapest way of reservoir characterization. Although it provides the most accurate option for finding distances from well to faults/discontinuities, reservoir characteristics and geology speed up or delay the transient wave travel time, leading to erroneous interpretations when isotropic methods are used.

Most of the well test methods to estimate the distance from wells to linear boundaries are presented for isotropic cases. In the semilog plot, a fault is detected when the slope of the radial flow regime doubles its value. The intercept of lines going through these two semilog lines are normally used to find the distance from the well to the fault. Among the isotropic methods, the following can be named: [8,9,17,20], MDH presented by [2,3,6,7,16,18,21,22], Sabet presented by

**How to cite:** Escobar, F.H., Bonilla, L.F. and Hernández, C.M., A practical calculation of the distance to a discontinuity in anisotropic systems from well test interpretation. DYNA, 85(207), pp. 65-73, Octubre - Diciembre, 2018.

© The author; licensee Universidad Nacional de Colombia.   
Revista DYNA, 85(207), pp. 65-73, Octubre - Diciembre, 2018, ISSN 0012-7353  
DOI: <http://doi.org/10.15446/dyna.v85n207.72281>

[24] and [24]. [13] compiled the methods produced until 1970.

Regarding the application of the pressure derivative, the work by [4] presented a new mathematical solution for a linear boundary detection, including wellbore storage and skin factor. The authors also developed a type-curve matching procedure and verified its application with a synthetic example. The first *TDS* Technique, [25], approach to find the distance from the well to a given linear discontinuity was presented by [19]. To estimate fault-to-well distance, they used the time at which radial flow regime ends.

[23] were the first to include fault detection in anisotropic reservoirs. Although they used conventional analysis (intersection of semilog lines) for the interpretation, new expressions for determining actual well image location and true distance were included. Later, [14] and [15], based on the work by [23], developed a new mathematical solution, including wellbore storage and skin factor. They provided both *TDS* Technique and type-curve matching interpretation techniques. Once the fault distance is found, the true distance—corrected by anisotropy effects—is obtained using the formulae of [23].

This work is also based on the works of [15] and [23]. A more general and practical formula was also developed using the time at which the radial flow regime ends. However, this new formula includes the effects of both anisotropy angle and anisotropy index. It was obtained by creating a unified behavior of pressure derivative against  $\theta_{FC} t_D / (I_A^{0.5} L_f^2)$ , where  $\theta_{FC}$  is a correction factor involving the anisotropy angle and  $I_A$  is the areal anisotropy index ( $k_x/k_y$ ). When the ending time of the radial flow regime is obscured by noise, the inflection point observed between the two pressure derivative plateaus is used in a similar equation. However, this inflection point is better determined using the maximum point on the second pressure derivative curve. For the case of a constant-pressure boundary, a negative unit slope line is developed. An equation for such a line was empirically (linear regression) obtained, so an arbitrary point read on such a line is used to find the distance from the well to the discontinuity. Also, the intersect of such a line with the extension of the radial flow regime line is used to develop another expression to find the distance to the constant-pressure boundary. Synthetic examples and a field case were used to successfully verify the developed equations. Care must be taken if an anisotropic reservoir is dealt with as an isotropic system, since the error could be as high as 100%.

## 2. Mathematical model

The classic assumptions used in well test analysis also apply here; this means that, regardless of gravity, a single and slightly compressible fluid with constant viscosity, a homogeneous porous medium and maximum permeability and minimum permeability are oriented in the  $x$  and  $y$  directions, respectively, the  $x$ - $y$  coordinate system can be transformed by changing the scale along each axis:

$$\bar{x} = x \quad (1)$$

$$\bar{y} = y\sqrt{I_A} \quad (2)$$

Thus,  $I_A$  the anisotropic index or horizontal permeability ratio, is defined by the following:

$$I_A = k_x / k_y \quad (3)$$

The method of images, [5], can be applied once the coordinate change is achieved to convert to isotropic conditions. [23] presented a general well imaging technique based on Eqs. (1) and (2), so actual image well location is given by the following:

$$x_I = \frac{L_f 2I_A \cos \theta}{I_A \cos^2 \theta + \sin^2 \theta} \quad (4)$$

$$y_I = \frac{L_f 2 \sin \theta}{I_A \cos^2 \theta + \sin^2 \theta} \quad (5)$$

These equations imply that the well image location in an anisotropic medium is a function of both the anisotropy index and the angle formed by the fault and the principal permeability axis. Isotropic system results whenever the fault is normal to either principal axis ( $\theta = 0$  or  $\pi/2$ ) as demonstrated by [23]. Who also provided A better picture is given in Fig. 1, and a detailed development of Eqs. (4) and (5) is presented by [23]. Using these equations, they also arrived at the following:

$$L_f = (L_f)_{app} / \sqrt{I_A \left[ I_A \left( \frac{\cos \theta}{I_A \cos^2 \theta + \sin^2 \theta} \right)^2 + \left( \frac{\sin \theta}{I_A \cos^2 \theta + \sin^2 \theta} \right)^2 \right]} \quad (6)$$

Where  $(L_f)_{app}$  is the apparent or uncorrected well-to-fault distance found for the isotropic system case. Estimation of well pressure behavior is obtained once the image well location is determined. The denominator of Eq. (6) can be read from Fig. 9 by [23]. [15] provided a general solution, including wellbore storage and skin factor, for a well near either a sealing fault or a constant-pressure boundary. This solution avoids setting many well images.

$$P_{wD}(1, t_D) = P_{wD}(1, t_D) \pm P_D(r_D, t_D) \quad (7)$$

Being that

$$r_D = \frac{2L_f}{r_w}; \quad r_w \leq L_f \leq \infty \quad (8)$$

The  $\pm$  symbol in Eq. (7) considers the solution for either the fault or constant-pressure boundary. When the sign is positive, a sealing fault is near the well. When the sign is negative, a constant-pressure boundary is then set, and radial stabilization characterized by a negative-unit slope in the pressure derivative curve is presented once the constant-pressure boundary is felt by the transient wave. Radial

stabilization has been characterized by [11] and [12]. The two terms at the right side of Eq.(7) are defined by the following:

$$\bar{P}_D(1, s) = \frac{K_0(\sqrt{s}) + S\sqrt{s}K_1(\sqrt{s})}{s\{sC_D[K_0(\sqrt{s}) + S\sqrt{s}K_1(\sqrt{s})] + \sqrt{s}K_1(\sqrt{s})\}} \quad (9)$$

$$\bar{P}_D(r_D, s) = \frac{K_0(\sqrt{sr_D})}{s\{sC_D[K_0(\sqrt{s}) + S\sqrt{s}K_1(\sqrt{s})] + \sqrt{s}K_1(\sqrt{s})\}} \quad (10)$$

### 3. Interpretation methodology

The *TDS* Technique, [25], is a powerful and practical interpretation technique that uses characteristic lines and features found on the pressure derivative plot. The solutions of the diffusivity equation for each individual flow regime are used to develop mathematical expressions to determine reservoir parameters. Maximum points, minimum points and inflection points are also used to develop equations for further reservoir characterization or parameter verification. Even though the intersection of the governing equations of two given flow regimes do not have any physical meaning, its use also allows further expressions to be developed to create more equations.

Let us start by defining some dimensional quantities for oil reservoirs:

$$t_D = \frac{0.0002637\bar{k}t}{\phi\mu c_w r_w^2} \quad (11)$$

The dimensionless pressure and pressure derivative follow:

$$P_D = \frac{\bar{k}h\Delta P}{141.2q\mu B} \quad (12)$$

$$t_D * P_D' = \frac{\bar{k}h(t * \Delta P')}{141.2q\mu B} \quad (13)$$

The application of Eq.(7) leads to several pressure derivatives versus time behaviors, as displayed in Figs. 2 through 5. As can be seen, a variety of derivatives and, of course, pressure responses are obtained as the parameters are varied. This makes the application of type-curve matching difficult, as proposed by [15]. [15] also extended the *TDS* Technique for anisotropic systems but they involved an expression for the estimation of the true well-to-discontinuity distance with Eq.(6), presented by [23]. A more practical application of the *TDS* Technique will be developed here.

Fig. 1 presents the pressure derivative behavior for three different well-to-fault distances in isotropic systems. A unique behavior for the three systems is required to obtain the characteristic points that will be used to develop the interpretation equations. Notice in Fig. 1 that the dimensionless time at which the fault is felt increases as the well-fault distance increases; then, for the behavior unification, the dimensionless time is divided by the distance,

$L_f^n$ , where  $n$  is an unknown exponent that may affect the unified behavior. Although, not shown here, when  $n = 1$ , no unified behavior is obtained; then,  $n$  must be different than one and ought to be determined. A simple procedure to find  $n$  is based on the use of the pressure derivative curve with  $L_f = 1$  ft.; in such a case,  $n$  has no impact on the pressure derivative curve, since a division by the unity does not cause any alteration on the result (see Fig. 5). To find the value of  $n$ , an arbitrary point is chosen during the time between the two plateaus seen on the pressure derivative, which is the matching zone of interest on the curve  $L_f = 1$  ft. The arbitrary chosen reference point was the inflection point. An analogous point is taken from another curve with  $L_f > 1$ . For this case, the arbitrary curve for  $L_f = 1500$  ft. was chosen. The reading points are then obtained from Figs. 2 and 6:

$$(t_D * P_D')_{\text{inf}} = 0.681097 \quad (t_D)_{\text{inf}} [\text{for } L_f = 1500 \text{ ft}] = 24647408.81 \\ (t_D)_{\text{inf}} [\text{for } L_f = 1 \text{ ft}] = 10.9544$$

Therefore, the following matching expression is given:

$$\frac{t_D}{L_f^n} \Big|_{L_f=1 \text{ ft}} = \frac{t_D}{L_f^n} \quad (14)$$

Which can easily be written as

$$t_D \Big|_{L_f=1 \text{ ft}} = \frac{t_D}{L_f^n} \Big|_{L_f=1500 \text{ ft}} \quad (15)$$

Replacing the reading values from Figs. 2 and 6.

$$10.9544 = \frac{24647408.81}{1500^n} \quad (16)$$

Then,  $n = 2$  is determined using Eq.(16). Therefore, after dividing the dimensionless time of Fig. 1 by  $L_f^2$ , a unique curve, as given in Fig. 4, will be obtained.

A similar treatment was first performed on Fig. 2 for the anisotropy index. As seen on that plot, the inflection point increases as the anisotropy index increases its effect in the denominator. An  $n$  value of 0.5 was found with a procedure similar to the one used for the well-to-fault distance case. In Fig. 3, the effect of the anisotropy angle,  $\theta$ , is presented. As  $\theta$  increases, the inflection point shows up earlier, meaning that its effect goes in the numerator. The  $n$  exponent for this case is the unity, but the effect changes when  $\theta \geq \pi/2$ . Then, finally, the unified behavior is obtained when the dimensionless time is multiplied by a correction factor,  $\theta_{FC}$ , and divided by the product of the square root of the anisotropy index times the squared well-to-fault distance. The range of angles applied for  $\theta_{FC}$  is given in Eq.(19). This also works for the constant-pressure boundary case, as shown in Fig. 4. Fig. 6 presents a unified dimensionless pressure derivative behavior against  $\theta_{FC} t_D / (I_A^{0.5} L_f^2)$ . In other words, universal dimensionless pressure derivative behavior is obtained. From that plot, the inflection time,  $t_{\text{inf}}$ —once the fault has been felt—for all cases is given by the following:

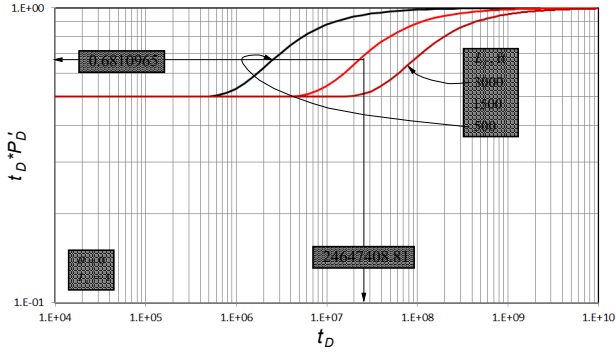


Figure 1. Effect of fault-well distance,  $L_f$ , on the pressure derivative behavior for isotropic systems  
Source: Authors

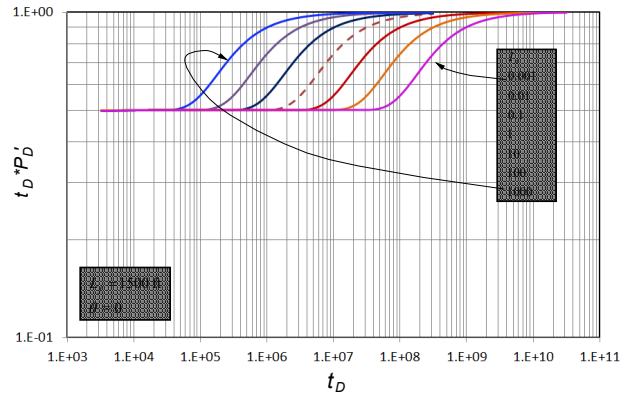


Figure 2. Effect of anisotropy index,  $I_A$ , on the pressure derivative behavior for anisotropic systems;  $\theta = 0$  and  $L_f = 1500$  ft.  
Source: Authors

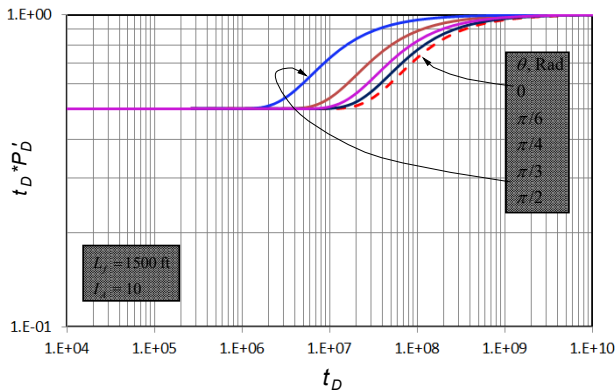


Figure 3. Effect of anisotropy angle on the pressure derivative behavior for anisotropic systems;  $I_A = 10$  and  $L_f = 1500$  ft.  
Source: Authors

$$(t_D)_{\text{inf}} = \frac{0.0002637 \theta_{FC} \bar{k} t_{\text{inf}}}{I_A^{0.5} \phi \mu c_i L_f^2} = 0.981 \quad (17)$$

The distance from the well to the linear boundary is obtained from the following:

$$L_f = \frac{1}{60.993} \sqrt{\frac{\theta_{FC} \bar{k} t_{\text{inf}}}{I_A^{0.5} \phi \mu c_i}} \quad (18)$$

The anisotropy angle correction factor,  $\theta_{FC}$ , is given by the below:

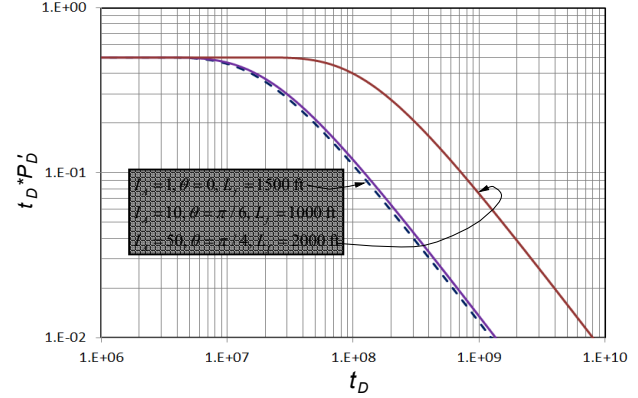


Figure 4. Mixed effect of anisotropy index,  $I_A$ ; anisotropy angle,  $\theta$ , and discontinuity-well distance,  $L_f$ , on the pressure derivative behavior for an anisotropic system  
Source: Authors

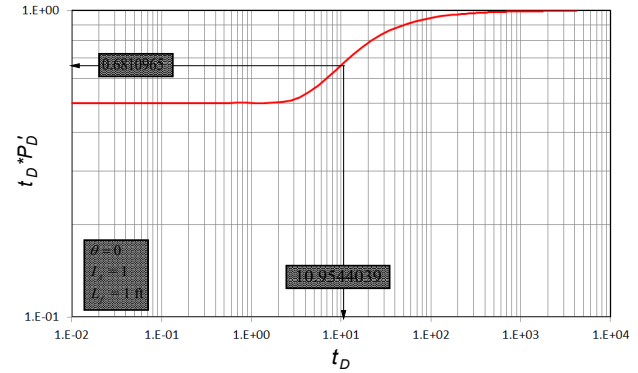


Figure 5. Pressure derivative behavior for isotropic systems;  $L_f = 1$  ft.  
Source: Authors

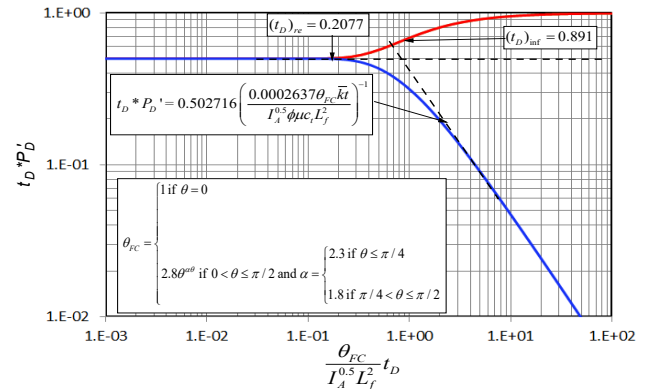


Figure 6. Unified pressure derivative behavior for anisotropic system with different values of anisotropy index,  $I_A$ ; anisotropy angle,  $\theta$ , and discontinuity-well distance,  $L_f$   
Source: Authors

$$\theta_{FC} = \begin{cases} 1 & \text{if } \theta = 0 \\ 2.8\theta^{\alpha\theta} & \text{if } 0 < \theta \leq \pi/2 \text{ and } \alpha = \begin{cases} 2.3 & \text{if } \theta \leq \pi/4 \\ 1.8 & \text{if } \pi/4 < \theta \leq \pi/2 \end{cases} \end{cases} \quad (19)$$

For the sealing-fault case, the inflection time is better obtained using the maximum point obtained on the second pressure derivative curve.

It is also shown in Fig. 6 that the radial flow regime ends at a dimensionless time of 0.2077, meaning

$$\frac{\theta_{FC}}{I_A^{0.5} L_f^2} (t_D)_{re} = 0.2077 \quad (20)$$

Replacing Eq.(11) in the above equation leads to

$$\frac{0.0002637\theta_{FC}\bar{k}t_{re}}{I_A^{0.5}\phi\mu c_t L_f^2} = 0.2077 \quad (21)$$

From which the below is developed:

$$L_f = \frac{1}{25.0142} \sqrt{\frac{\theta_{FC}\bar{k}t_{re}}{I_A^{0.5}\phi\mu c_t}} \quad (22)$$

This is very close to the expression given by Guira et al. (2002) for an isotropic case:

$$L_f = \frac{1}{24.06} \sqrt{\frac{\bar{k}t_{re}}{\phi\mu c_t}} \quad (23)$$

As observed in Figs. 5 and 7, the constant-pressure single-boundary case has an especial feature. Radial stabilization develops once the boundary has been reached by the transient wave, and the pressure derivative curve displays a negative unit-slope line. After the unification of the dimensionless pressure derivative curve, the governing equation for such a line obtained from the regression analysis is

$$(t_D^* P_D')_{nus} = 0.311 \left( \frac{\theta_{FC} t_{D_{nus}}}{I_A^{0.5} L_f^2} \right)^{-1} \quad (24)$$

Where  $r_{nusi}$  stands for radial negative unit-Slope intersection. Replacing the dimensionless quantities given by Eqs. (11) and (13) in Eq.(24) and solving for the well-to-discontinuity distance yields the following:

$$L_f = \frac{\bar{k}}{408.0774\mu} \sqrt{\frac{h\theta_{FC} t_{nus} (t^* \Delta P')_{nus}}{qB I_A^{0.5} \phi c_t}} \quad (25)$$

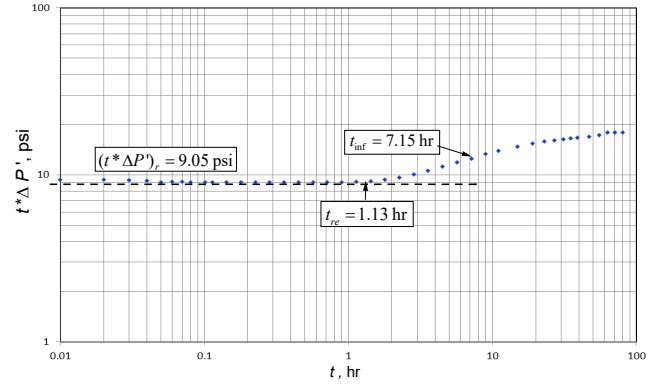


Figure 7. Pressure derivative versus time log-log plot for example 1  
Source: Authors

The point of intersection between the radial flow regime line and the radial stabilization negative unit-slope line is a unique feature; by equating the right side of Eq.(24) to one half and solving for the well-to-discontinuity distance, it is obtained:

$$L_f = \frac{1}{48.567} \sqrt{\frac{\theta_{FC} \bar{k} t_{r_{nusi}}}{I_A^{0.5} \phi \mu c_t}} \quad (26)$$

Finally, the reservoir permeability is found from an expression given by Tiab (1995):

$$\bar{k} = \sqrt{k_x k_y} = \frac{70.6 q \mu B}{h(t^* \Delta P')_r} \quad (27)$$

The gas equations are provided in appendix A.

## 4. Examples

### 4.1. Synthetic example 1

Using the data given in Table 1 and the pressure derivative plot of Fig. 7, find the distance from the well to a sealing fault.

**Solution.** The following information was read from Fig. 7.

$$(t^* \Delta P')_r = 9.05 \text{ psi} \quad t_{re} = 1.13 \text{ hr} \\ t_{inf} = 7.15 \text{ hr}$$

Find reservoir permeability using Eq.(27):

$$\bar{k} = \sqrt{k_x k_y} = \frac{70.6(500)(2.5)(1.23)}{(30)(9.05)} = 119.94 \text{ md}$$

Find the anisotropy angle factor using Eq.(19):

$$\theta_{FC} = 2.8\theta^{1.8\theta} = 2.8(\pi/6)^{1.8(\pi/6)} = 1.28456$$

Find the well-fault distance using Eqs. (18) and (22):

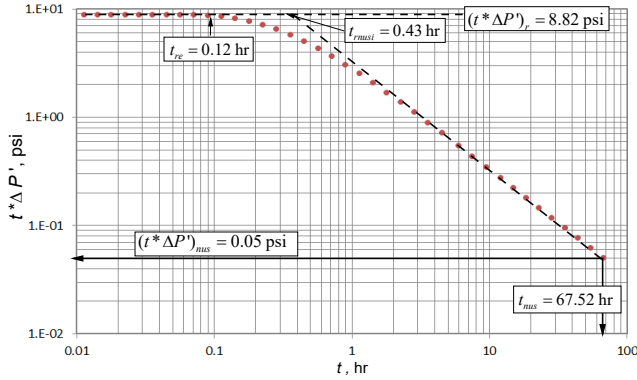


Figure 8. Pressure derivative versus time log-log plot for example 2  
Source: Authors

Table 1.  
Reservoir and fluid data for examples

PARAMETER	Example 1	Example 2	Field Case
$r_w$ , ft.	0.5	0.3	0.3
$h$ , ft.	100	30	70
$\phi$ , %	15	20	12
$I_A$ , md	18	30	5
$\bar{k}$ , md	120	250	92.53
$\theta$ , Rad	$\pi/6$	$5\pi/12$	$\pi/6$
$q$ , bbl/D	500	250	550
$B$ , rb/STB	1.23	1.25	1.324
$c_h$ , 1/psi	$1 \times 10^{-6}$	$1 \times 10^{-6}$	$1.328 \times 10^{-5}$
$\mu$ , cp	2.5	3	1.26
$L_f$ , ft	415	278	

Source: Authors

$$L_f = \frac{1}{60.993} \sqrt{\frac{(1.28456)(120)(7.15)}{(18^{0.5})(0.15)(2.5)(1 \times 10^{-6})}} = 431.5 \text{ ft}$$

$$L_f = \frac{1}{25.0142} \sqrt{\frac{(1.28456)(120)(1.13)}{(18^{0.5})(0.15)(2.5)(1 \times 10^{-6})}} = 418.3 \text{ ft}$$

If the system were isotropic, the well-fault distance would be estimated with Eq. (23).

$$L_f = \frac{1}{24.06} \sqrt{\frac{(120)(1.13)}{(0.15)(2.5)(1 \times 10^{-6})}} = 790.35 \text{ ft}$$

#### 4.2. Synthetic example 2

Find the distance from the well to a constant-pressure linear boundary using the data given in Table 1 and the pressure derivative plot of Fig. 8.

**Solution.** The following data were taken from Fig. 8.

$$\begin{aligned} (t^* \Delta P')_r &= 8.82 \text{ psi} & t_{re} &= 0.12 \text{ hr} \\ t_{musi} &= 0.43 \text{ hr} \\ t_{mus} &= 67.52 \text{ hr} & (t^* \Delta P')_{mus} &= 0.05 \text{ psi} \end{aligned}$$

Reservoir permeability is found with Eq.(27), and the anisotropy angle factor is found using Eq.(19):

$$\bar{k} = \sqrt{k_x k_y} = \frac{70.6(250)(3)(1.25)}{(100)(8.82)} = 250.15 \text{ md}$$

$$\theta_{FC} = 2.8\theta^{1.8\theta} = 2.8(5\pi/12)^{1.8(5\pi/12)} = 5.28066$$

Find the distance from the well to the linear boundary using Eqs. (22), (25) and (26):

$$L_f = \frac{1}{25.0142} \sqrt{\frac{(5.28066)(250)(1.13)}{(30^{0.5})(0.2)(2.5)(1 \times 10^{-6})}} = 270.62 \text{ ft}$$

$$L_f = \frac{250}{408.0774(3)} \sqrt{\frac{(39)(5.28066)(67.52)(0.05)}{(250)(1.25)(30^{0.5})(0.2)(1 \times 10^{-6})}} = 255.3 \text{ ft}$$

$$L_f = \frac{1}{48.567} \sqrt{\frac{(5.28066)(250)(0.12)}{(30^{0.5})(0.2)(2.5)(1 \times 10^{-6})}} = 277.6 \text{ ft}$$

If the system were isotropic, the distance from the well to the linear boundary would be estimated to be the following by using Eq.(23):

$$L_f = \frac{1}{24.06} \sqrt{\frac{(250)(0.12)}{(0.2)(3)(1 \times 10^{-6})}} = 556.33 \text{ ft}$$

#### 4.3. Field example

[14] presented field data for a pressure test run in a well near a sealing fault in an anisotropic system. Pressure and pressure derivative versus time data are provided in Fig. 9. Finding the distance from well to the fault is required.

**Solution.** The following information was taken from Fig. 9.

$$t_{re} = 3 \text{ hr} \quad t_{inf} = 13 \text{ hr}$$

Find the anisotropy angle factor using Eq.(19):

$$\theta_{FC} = 2.8\theta^{1.8\theta} = 2.8(\pi/6)^{1.8(\pi/6)} = 1.28456$$

Find the well-fault distance using Eqs. (18) and (22):

$$L_f = \frac{1}{60.993} \sqrt{\frac{(1.28456)(92.53)(18)}{(5^{0.5})(0.12)(1.26)(1.328 \times 10^{-5})}} = 357.9 \text{ ft}$$

$$L_f = \frac{1}{25.0142} \sqrt{\frac{(1.28456)(92.53)(3)}{(5^{0.5})(0.12)(1.26)(1.328 \times 10^{-5})}} = 356.3 \text{ ft}$$

If the system were isotropic, the well-to-fault distance would be estimated using Eq.(23).



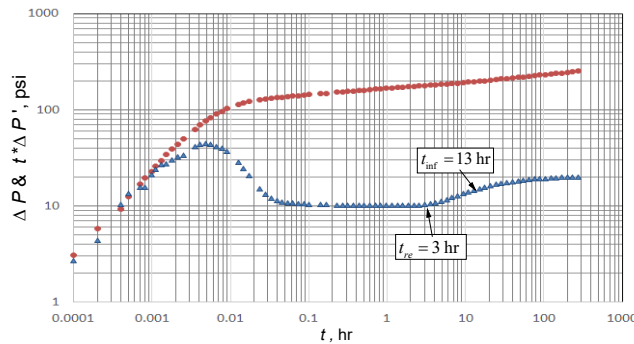


Figure 9. Pressure derivative versus time log-log plot for the field example  
Source: Authors

Table 2.  
Deviation errors from the working examples

Example 1, $L_f = 415$ ft.			Field Example 1, $L_f = 370$ ft. <sup>(*)</sup>		
Eq.	$L_f$ , ft.	Abs. Error, %	Eq.	$L_f$ , ft.	Abs. Error, %
18	431.5	3.97	18	357.9	3.3
22	418.3	0.80	22	356.3	3.7
23	790.35	90.45	23	488.7	32.1
Example 2, $L_f = 278$ ft.					
Eq.	$L_f$ , ft.	Abs. Error, %			
22	270.62	2.65			
25	255.30	8.17			
26	277.60	0.14			
23	556.33	100.12			

(\*) Commercial interpretation software  
Source: Authors

$$L_f = \frac{1}{24.06} \sqrt{\frac{(92.53)(3)}{(0.12)(1.26)(1.328 \times 10^{-5})}} = 488.7 \text{ ft}$$

[14] estimated  $L_f = 462.24$  ft. The authors corrected the apparent distance estimated with Eq.(23) by using a reading from Fig. 9 by [23]. We found, however, that the correction factor was not estimated well. Then, we interpreted the test with a commercial software and found the well-to-fault distance to be 370 ft. This value was then used as our reference value for the estimation of the error.

## 5. Discussion of results

Table 2 provides the deviation error obtained for the working exercises. The proposed equations provided error values lower than 4%. The higher error was obtained from Eq.(25), which uses any point on the negative unit slope line.

It is important to remark that the estimations provide deviation errors higher than 30% for the actual field case and even higher than 90% for the synthetic examples when the system is dealt as an isotropic case.

## 6. Conclusions

1. Practical and accurate expressions using the unique features of the pressure derivative plot were developed

to determine the distance from a well to a linear boundary (constant-pressure or sealing fault) in areal anisotropic reservoirs. The expressions—successfully tested with two simulated examples and one field case example—simultaneously involve the anisotropy angle and the anisotropic index. Most of the developed expressions provided errors lower than 4%, except for one expression that uses an arbitrary point on the negative-unit-slope line.

2. The pressure derivative as a function of  $\theta_{FC} t_D / (I_A^{0.5} L_f^{0.5})$  always displays the same behavior for wells near a linear boundary. The anisotropy angle factor,  $\theta_{FC}$ , has different estimations if the angle is less or higher than  $45^\circ$ . The relationship  $\theta_{FC} t_D / (I_A^{0.5} L_f^{0.5})$  forms the basis of the methodology developed in this work.
3. Determination of the well-discontinuity distance using the isotropic formulae can provide errors even higher than 100%. For the real example, the error was 32%.

## References

- [1] Agarwal, R.G., Real gas pseudo-time - a new function for pressure buildup analysis of MHF gas wells. Society of Petroleum Engineers, 1979. DOI: 10.2118/8279-MS.
- [2] Bixel, H.C., Larkin, B.K. and Van-Poolen, H.K., Effect of linear discontinuities on pressure build-up and drawdown behavior. Journal of Petroleum Technology, pp. 85, Society of Petroleum Engineers, 1963. DOI: 10.2118/611-PA.
- [3] Bixel, H.C. and Van-Poolen, H.K., Pressure drawdown and build-up in the presence of radial discontinuities. Society of Petroleum Engineers, 1967. DOI: 10.2118/1516-PA.
- [4] Chu, L. and Grader, A.S., A new technique for linear boundary detection with wellbore storage and wellbore skin. Society of Petroleum Engineers, 1991. DOI: 10.2118/22683-MS.
- [5] Collins, R.E., Flow of fluids through porous materials. Reinhold Publishing Corp, New York, 1961, 270 P.
- [6] Davis, E.G. and Hawkins, M.F., Linear fluid-barrier detection by well pressure measurements (includes associated discussion and reply). Society of Petroleum Engineers, 1963. DOI: 10.2118/462-PA.
- [7] Dolan, J.P., Einarsen, C.A. and Hill, G.A., Special applications of drill-stem test pressure data. Society of Petroleum Engineers, 1957.
- [8] Earlougher, R.C., Advances in well test analysis. Monograph Series, 5, SPE, Second Printing, Dallas, TX, 1977.
- [9] Earlougher, R.C. and Kazemi, H., Practicalities of detecting faults from buildup testing. Society of Petroleum Engineers, 1980. DOI: 10.2118/8781-PA.
- [10] Escobar, F.H., López, A.M. and Cantillo, J.H., Effect of the pseudotime function on gas reservoir drainage area determination. CT&F – Ciencia, Tecnología y Futuro, 3(3), pp. 113-124, 2007.
- [11] Escobar, F.H., Hernandez, Y.A. and Tiab, D., Determination of reservoir drainage area for constant-pressure systems using well test data. CT&F – Ciencia, Tecnología y Futuro, 4(1), pp. 51-72, 2010.
- [12] Escobar, F.H., Ghisays-Ruiz, A. and Srivastava, P., Characterization of the spherical stabilization flow regime by transient pressure analysis. Journal of Engineering and Applied Sciences, 10(14), pp. 5815-5822, 2015.
- [13] Gibson, J.A. and Campbell, A.T., Calculating the distance to a discontinuity from D.S.T. data. Society of Petroleum Engineers, 1970. DOI: 10.2118/3016-MS.
- [14] Guira, B., Pressure behavior of a well in anisotropic reservoir near a no-flow boundary. MS Thesis, The University of Oklahoma, Norman, OK, 2001.
- [15] Guira, B., Tiab, D. and Escobar, F.H., Pressure Behavior of a Well in an Anisotropic Reservoir. Society of Petroleum Engineers, 2002. DOI: 10.2118/76772-MS.
- [16] Gray, K.E., Approximating well-to-fault distance from pressure build-up tests. Journal of Petroleum Technology, Society of Petroleum Engineers, 1965. DOI: 10.2118/968-PA.



- [17] Horner, D.R., Pressure Build-up in Wells, Proceedings of Third World Petroleum Congress – Section II, pp. 503-521, 1951.
- [18] Ishteiy, A.A. and Van-Poolen, H.K., Radius-of-drainage equation for pressure build-up. Society of Petroleum Engineers, 1969.
- [19] Ispas, V. and Tiab, D., New method of analyzing the pressure behavior of a well near multiple boundary systems. Society of Petroleum Engineers, 1999. DOI: 10.2118/53933-MS.
- [20] Kuchuk, F.J. and Kabir, S., Well test interpretation for reservoirs with a single linear no-flow barrier. Journal of Petroleum Science and Engineering, pp. 195-221, 1988. DOI: 10.1016/0920-4105(88)90011-3
- [21] Martinez-Romero, N. and Cinco-Ley, H., Detection of linear impermeable barriers by transient pressure analysis. Society of Petroleum Engineers, 1983. DOI: 10.2118/11833-MS.
- [22] Odeh, A.S., Flow test analysis for a well with radial discontinuity. Journal of Petroleum Technology, Society of Petroleum Engineers, pp. 328-334, 1969. DOI: 10.2118/2157-PA.
- [23] Overpeck, A.C. and Holden, W.R., Well imaging and fault detection in anisotropic reservoirs. Society of Petroleum Engineers, 1970. DOI: 10.2118/2731-PA.
- [24] Sabet, M., Well Testing. Gulf Publishing Co., First Printing, Houston, TX, USA. 1991, 460 P.
- [25] Tiab, D., Analysis of pressure and pressure derivative without type-curve matching: 1- skin and wellbore storage. Journal of Petroleum Science and Engineering, 12, pp. 171-181, 1995.

## Nomenclature

$B$	Volume factor, rb/STB
$C$	Wellbore storage coefficient, bbl/psi
$c_t$	Total system compressibility, psi <sup>-1</sup>
$DDR$	Dimensionless distance ratio
$h$	Reservoir thickness, ft.
$I_A$	Areal anisotropic ratio or permeability ratio
$\bar{k}$	Reservoir horizontal permeability, md
$k_x$	Reservoir permeability in the $x$ -direction, md
$k_y$	Reservoir permeability in the $y$ -direction, md
$L_f$	Distance from the well to the linear boundary, ft.
$n$	Undetermined exponent
$m(P)$	Pseudopressure, psi <sup>2</sup> /cp
$P$	Pressure, psi
$\bar{P}_D$	Dimensionless pressure in the Laplace space
$P_i$	Initial reservoir pressure, psi
$P_{wf}$	Wellbore flowing pressure, psi
$q$	Liquid flow rate, BPD
$q_g$	Gas flow rate, MSCF/D
$r_w$	Wellbore radius, ft.
$S$	Laplace parameter
$s$	Skin factor
$t$	Time, hr
$t_a(P)$	Pseudotime, hr-cp/psi
$t_D$	Dimensionless time
$t_{Da}$	Dimensionless pseudotime
$t_D * P_D'$	Dimensionless pressure derivative
$(t^* \Delta P')$	Pressure derivative
$x$	$x$ -direction
$y$	$y$ -direction

## Greeks Symbols

$\phi$	Porosity, fraction
$\mu$	Viscosity, cp
$\theta$	Angle, Rad
$\theta_{FC}$	Anisotropy angle correction factor

## Suffices

$app$	Apparent of uncorrected
$D$	Dimensionless
$i$	Initial
$I$	Image
$inf$	Inflection
$nus$	Negative unit slope
$r$	Radial
$re$	End of radial
$rnusi$	Intercept of the radial flow and the negative unit slope lines
$true$	True distance
$wf$	Well flowing
$ws$	Well static

## APPENDIX A. Gas Reservoirs

The dimensionless pseudopressure and pseudopressure derivative are defined by the following:

$$m(P)_D = \frac{\bar{k}h[m(P_i) - m(P)]}{1422.52q_g T} \quad (A.1)$$

$$t_D * m(P)'_D = \frac{\bar{k}h[t^* \Delta m(P)]}{1422.52q_g T} \quad (A.2)$$

[1] introduces the pseudotime function to account for the time dependence of both gas viscosity and total system compressibility:

$$t_a = \int_{t_0}^t \frac{dt}{\mu(t)c_t(t)} \quad (A.3)$$

This function is better defined as a pressure function given in hr psi/cp:

$$t_a(P) = \int_{P_0}^P \frac{(dt / dP)}{\mu(p)c_t(P)} dP \quad (A.4)$$

Now,  $\mu$  and  $c_t$  are pressure-dependent properties. Eq.(A.4) can be rewritten as follows:

$$t_D = \frac{0.0002637 \bar{k} t}{\phi(\mu c_t)_i r_w^2} \quad (A.5)$$

Including the pseudotime function,  $t_a(P)$ , in Eq.(A.5), the dimensionless pseudotime is given by the below:

$$t_{Da} = \left( \frac{0.0002637 \bar{k}}{\phi r_w^2} \right) t_a(P) \quad (A.6)$$

By multiplying and then dividing by  $(\mu c_t)_i$ , a similar Eq.to the

general dimensionless time expression, Eq.(27), can be obtained.

$$t_{Da} = \left( \frac{0.0002637k}{\phi(\mu c_t)_i r_w^2} \right) [(\mu c_t)_i \times t_a(P)] \quad (A.7)$$

With these new dimensionless quantities, Eqs. (1), (17), (20) and (21) will become the below:

$$L_f = \frac{1}{60.993} \sqrt{\frac{\theta_{FC} \bar{k} t_a(P)_{inf}}{I_A^{0.5} \phi}} \quad (A.8)$$

$$L_f = \frac{1}{25.0142} \sqrt{\frac{\theta_{FC} \bar{k} t_a(P)_{re}}{I_A^{0.5} \phi}} \quad (A.9)$$

$$L_f = \frac{\bar{k}}{1295.2521} \sqrt{\frac{h \theta_{FC} t_a(P)_{nus} [t^* \Delta m(P')]_{nus}}{qT I_A^{0.5} \phi}} \quad (A.10)$$

$$L_f = \frac{1}{48.567} \sqrt{\frac{\theta_{FC} \bar{k} t_a(P)_{musi}}{I_A^{0.5} \phi}} \quad (A.11)$$

The reservoir permeability, [10], is given by the following:

$$\bar{k} = \sqrt{k_x k_y} = \frac{711.26 q_s T}{h [t_a(P) * \Delta m'(P)]_r} \quad (A.12)$$

**F.H. Escobar**, he holds a BSc. degree from Universidad de America, and MSc. and PhD degrees from the University of Oklahoma, USA. All his degrees are in Petroleum Engineering. He is a professor and director of the research group GIPE in Universidad Surcolombiana, Neiva, Colombia. ORCID: 0000-0003-4901-6057.

**L.F. Bonilla**, he is a BSc. In Petroleum Engineer from Universidad Surcolombiana, and holds a MSc. degree in Petroleum Engineering from the University of Oklahoma, USA. Professor and member of the research group GIPE in Universidad Surcolombiana, Neiva, Colombia. ORCID: 0000-0002-6736-6811

**C.M. Hernández**, she holds a BSc. degree in Petroleum Engineering from Universidad Surcolombiana, she is a member of in Universidad Surcolombiana, Neiva, Colombia and works for Ecopetrol in Bogota, Colombia. ORCID: 0000-0002-1216-1018



UNIVERSIDAD NACIONAL DE COLOMBIA

SEDE MEDELLÍN  
FACULTAD DE MINAS

Área Curricular de Ingeniería  
Química e Ingeniería de Petróleos

Oferta de Posgrados

Maestría en Ingeniería - Ingeniería Química  
Maestría en Ingeniería - Ingeniería de Petróleos  
Doctorado en Ingeniería - Sistemas Energéticos

Mayor información:

E-mail: qcaypet\_med@unal.edu.co  
Teléfono: (57-4) 425 5317